NASA Balloon programs
AESOP-lite and ANITA

John Clem
University of Delaware

Ole Miss
Aug 10, 2017

ANITA

***An**tarctic Impulsive*
***T**ransient **A**ntenna*

Astrophysics
Ultra High Energy Neutrinos

AESOP-lite

***An**ti-**E**lectron **S**ub-**O**rbital*
***P**ayload- low energy*

Space Physics and Geomagnetic
Positrons and Electrons

Outline

NASA Balloon Program

Columbia Scientific Balloon Facility

Ballooning 101

ANITA and AESOP-lite payloads

Wallops Flight Facility
Goddard Space Flight Center

NASA Balloon Program

The primary objective of the NASA Balloon Program is to provide high altitude platforms for scientific and technological investigations.

These investigations include fundamental scientific discoveries that contribute to our understanding of the Earth, the Solar system, our Galaxy and the Universe.

Scientific balloons also provide a platform for the demonstration of potential new instrument and spacecraft technologies

Columbia Scientific Balloon Facility (CSBF)

Located in Palestine, Texas

CSBF, managed by the NASA Balloon Program, is a facility responsible for providing the launch, tracking and control, airspace coordination, telemetry and command systems, and recovery services for high altitude balloons.

Users of the CSBF include NASA centers, Universities, and scientific groups from all over the world.

A balloon flight involves both CSBF and the scientific team.

CSBF determines the launch site based on scientific goals, and provides local preparation facilities, balloons, launch and recovery vehicles, and personnel to support the logistical aspects of pre-flight, flight, and post flight activities.

Scientific team ship their payload to the launch site, and set up a field station to assemble their equipment, make last-minute preparations, and manage the experiment during flight.

Palestine, TX

Kiruna, Sweden

Active NASA Launch Sites

Alice Springs, Australia

Fort Sumner, NM

McMurdo, Antarctica

The General Anatomy of a NASA Balloon System

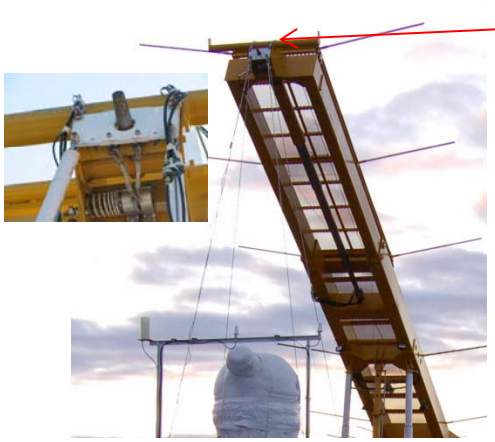

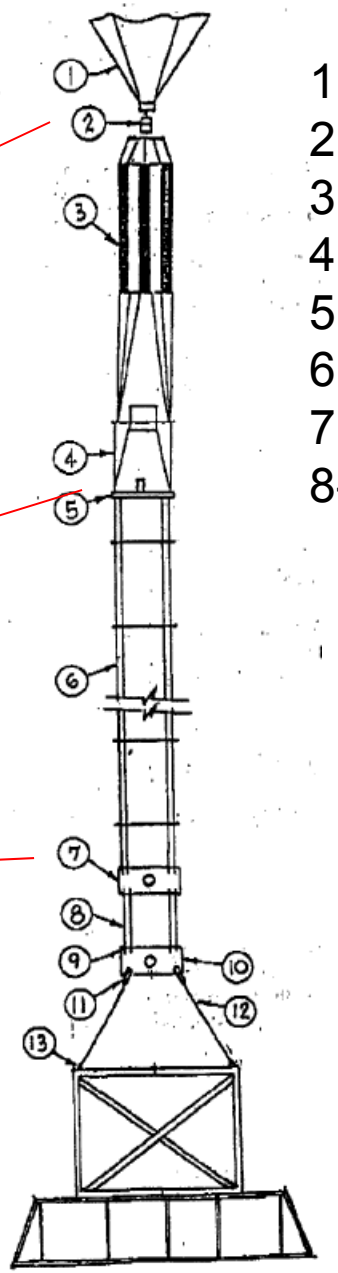

1. Balloon base
2. Balloon Terminate (separates balloon from parachute)
3. Parachute
4. Lower Chute Ring and cables
5. Parachute Separator (separates parachute from payload)
6. Flight Train or Cable Ladder
7. Crane Suspension Plate

8-13. Specific components to this payload

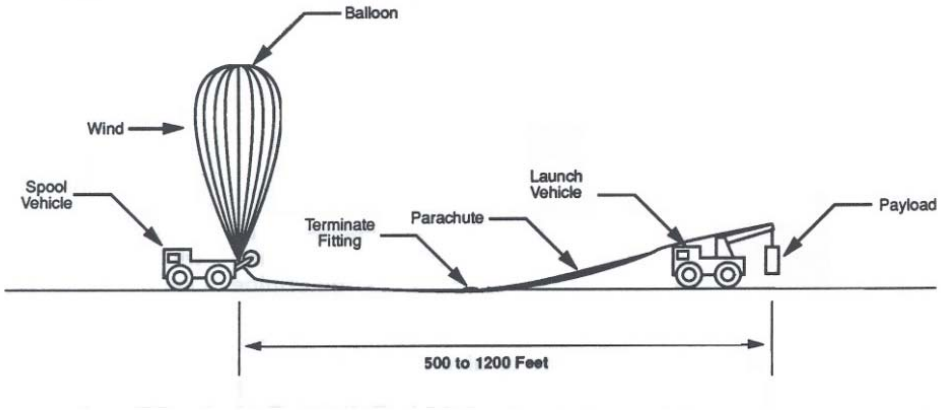

Payload at 140kft

Balloon is fully expanded at float altitudes

Flight Path Examples

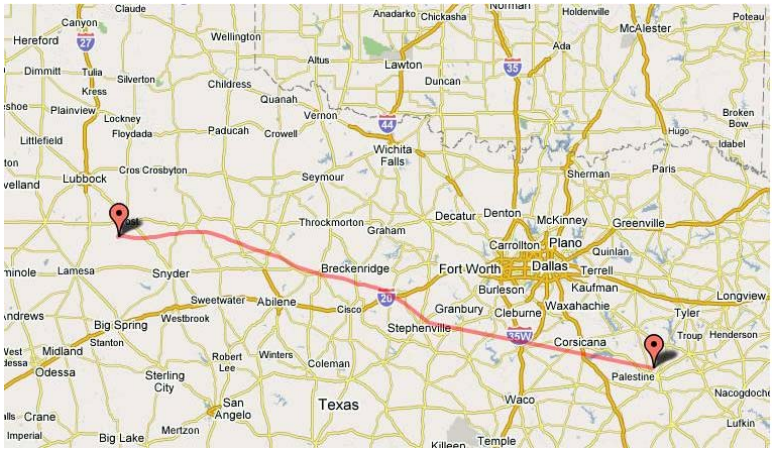

Palestine, Texas (Balloon facility site)

Kiruna, Sweden

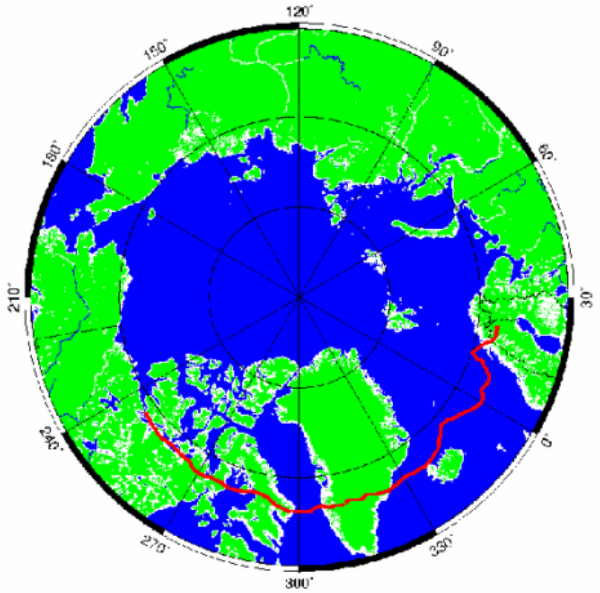

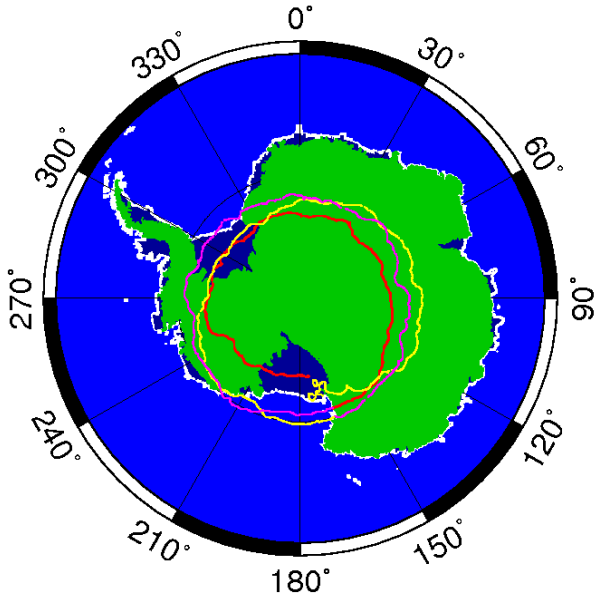

McMurdo, Antarctica

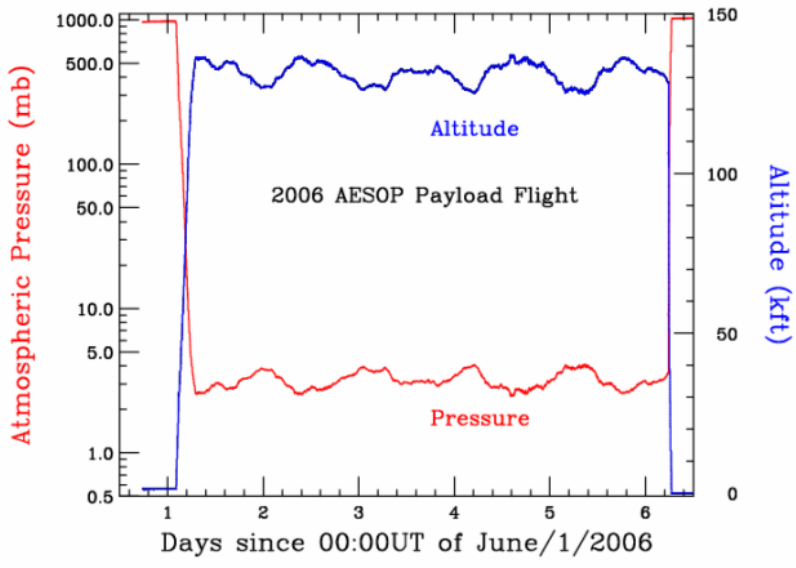

AESOP-lite

***An**ti-**E**lectron **S**ub-**O**rbital **P**ayload- Low Energy*

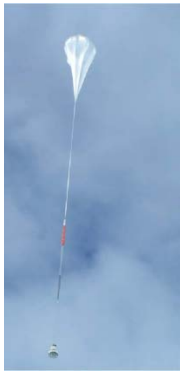

LEE payload 2011 Sweden

Team AESOP-lite

University of Delaware

John Clem - PI
Paul Evenson - CoI
Brian Lucas - Graduate Student
James Roth - Balloon Tech
Yang Zhou - Post-Doc

University of California Santa Cruz

Robert Johnson - CoI
Sarah Mechbal - Graduate Student

NASA

Dan Moses, Jeff Morrill and Jeff Newmark - Program Officers
Heliophysics Division
HTIDES Grant Number NNX15AL32G

Discovery of Cosmic rays occurred on a Balloon

As Hess's balloon ascended to 5300m, he observed the rate of ionization increased with altitude.

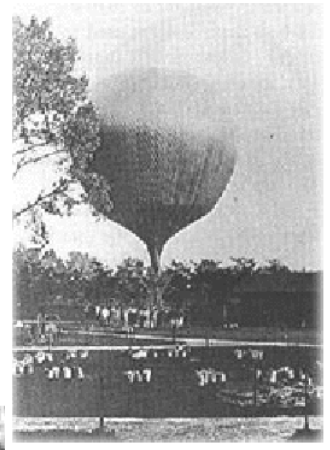

Hess lands following a historic 5,300 meter flight.
August 7, 1912
National Geographic photograph

He concluded, **"a radiation of very high penetrating power enters our atmosphere from above."**

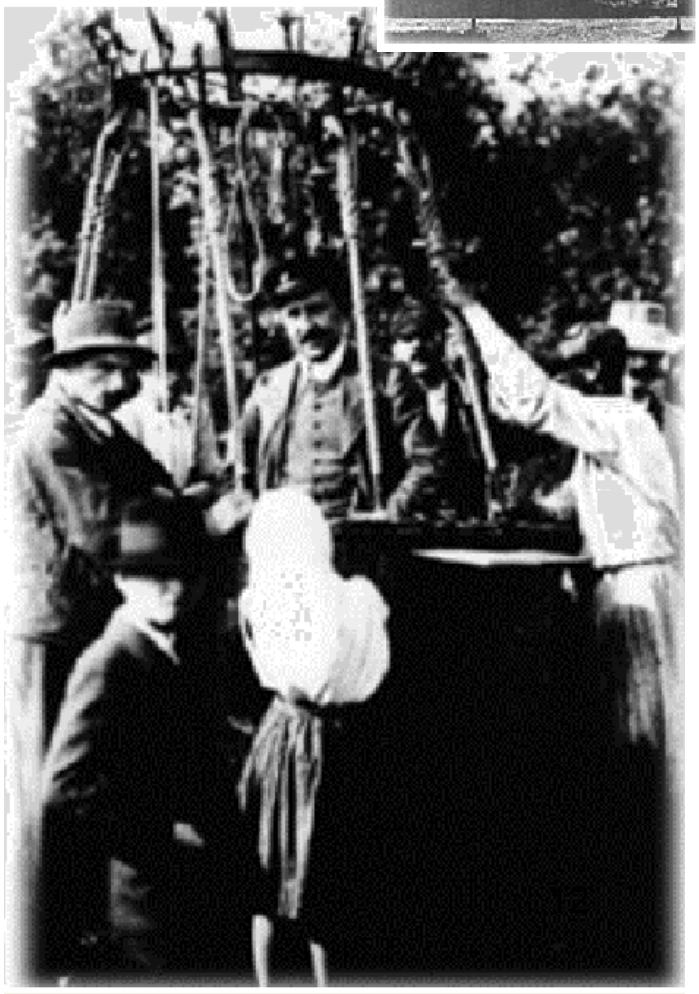

Initially Hess's theory about rays from space did not receive general acceptance, but increased research after World War I supported it. The newly discovered radiation was dubbed "Cosmic Rays" by Robert A. Millikan in 1925.

Today it is generally accepted the bulk of cosmic rays come from supernova explosions within our Galaxy.

Strong shock waves are generated from Super Nova

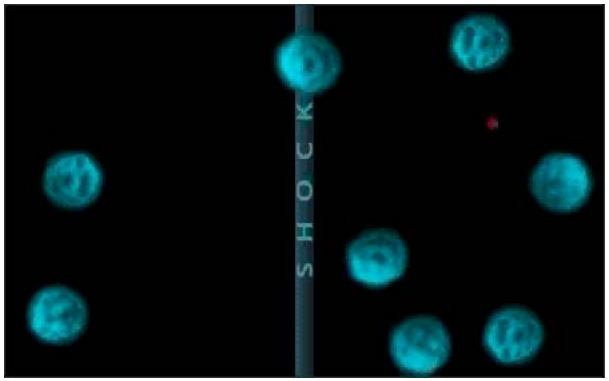

Rest frame of a shock wave

Fermi's 1st order shock acceleration theory predicts a power law spectrum.

Edge of the Heliosphere power index is
~ **-2.7** for nucleons
~ **-3.0** for electrons

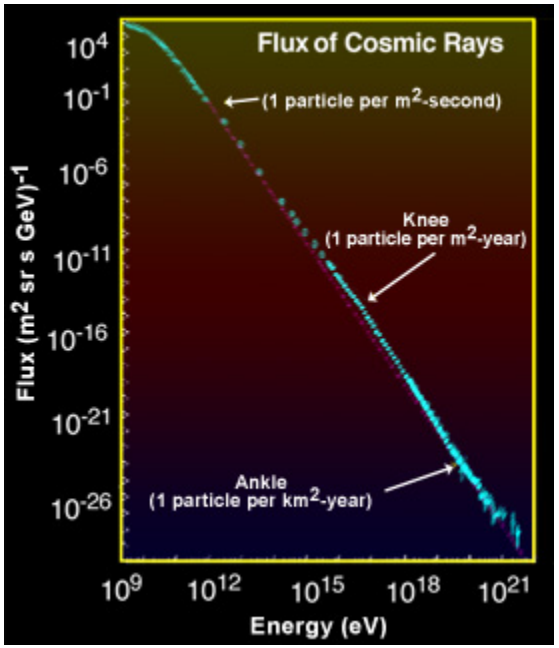

Local magnetic inhomogeneities (particle mirrors) are dragged by the shock
Particle acceleration occurs across the shock
(1st order Fermi Acceleration)

Arriving the edge of the heliosphere, Cosmic Rays encounter the Solar Wind, a low density stream of hot plasma emanating radially from the sun.

Solar Magnetic field or Interplanetary Magnetic Field (IMF) is embedded in the solar wind and carried outward.

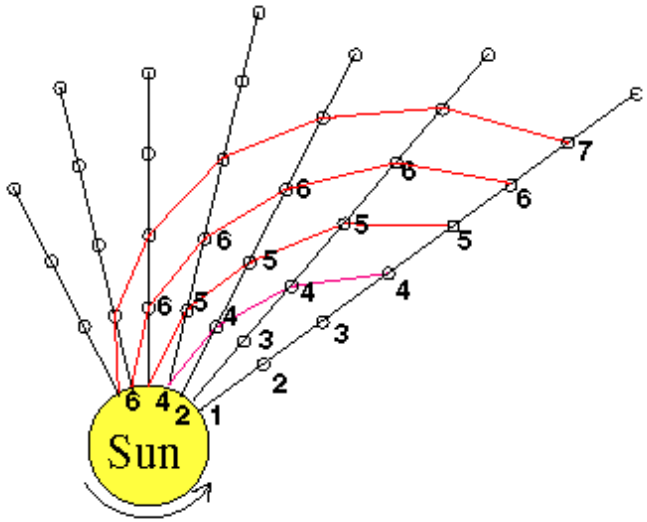

Combination of the outward flowing solar wind and the solar rotation (27days) produces a spiral geometry for the IMF
Parker Spiral)

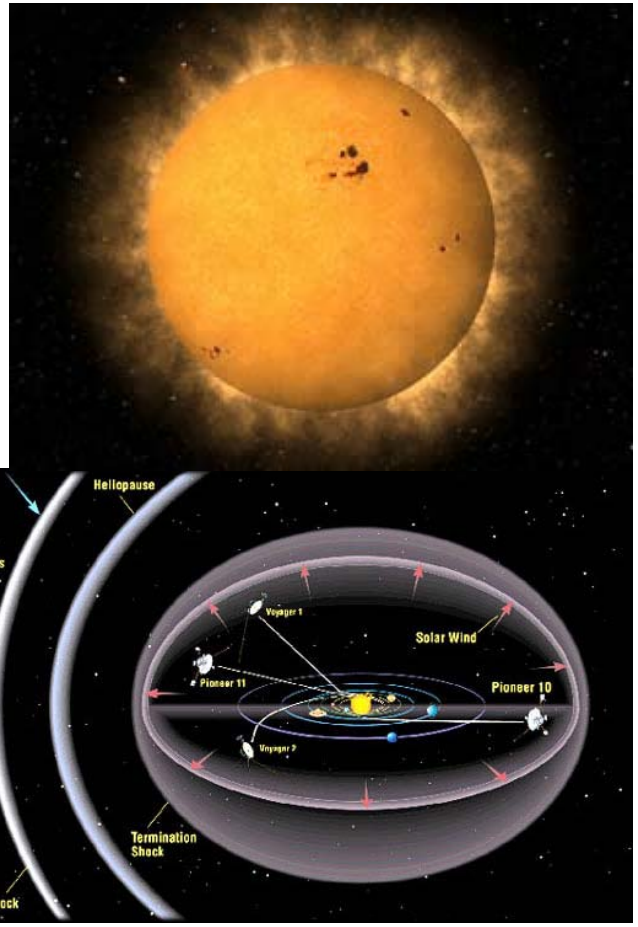

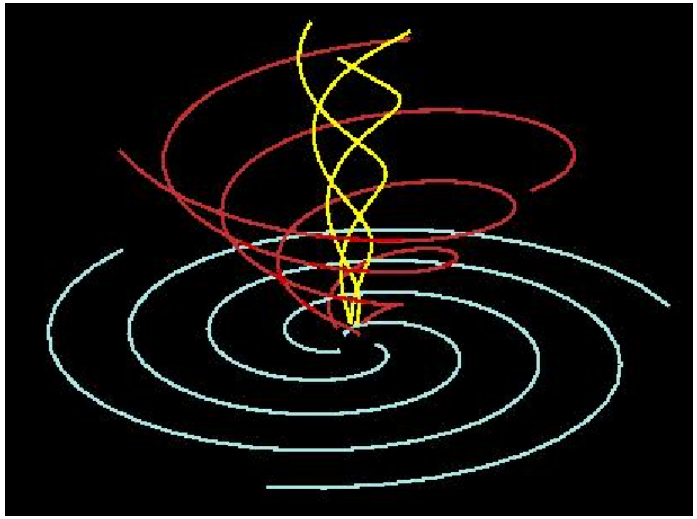

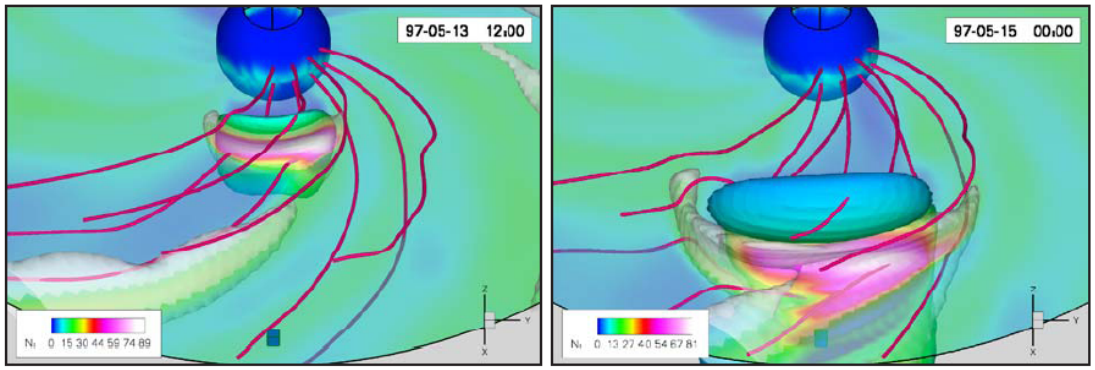

IMF lines are not always smooth. Rooted on the solar surface, a highly convective medium causing field lines to move around.

Solar flares or mass ejections produces turbulence in the solar wind resulting in major irregularities or scattering regions.

Cosmic Rays propagate along Parker spiral IMF and interact with these fluctuations altering the kinematics.

These magnetic fluctuations alters the nominal helical trajectory of cosmic rays

The observed spectrum of cosmic rays at Earth is strongly influence by the population density and amplitude distributions of magnetic fluctuations in the Heliosphere.

The level of Solar Activity, 11 year cycle, directly influences the characteristics of these fluctuations, and consequently affects the cosmic ray intensity at Earth.

This time variation in cosmic rays is referred to as **Solar Modulation.**

Number of observed sunspots (concentration of high magnetic flux) is typically a very good indicator of the level of solar modulation

Trajectory of charged particle in a smooth magnetic field

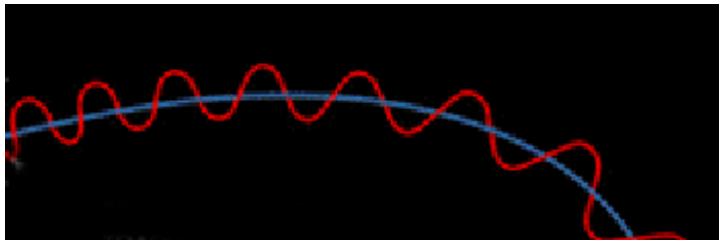

The angle between the direction of the magnetic field and a particle's spiral trajectory is referred to as the ***"pitch angle"***

11 year Cycle Animation
(rotation rate is scaled for viewing)

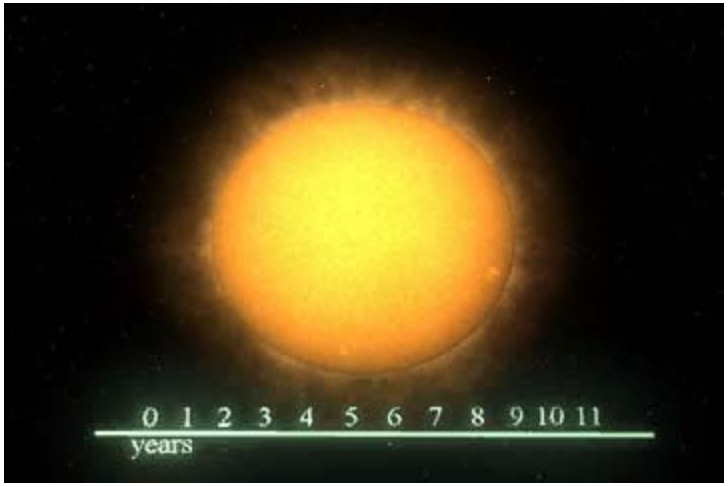

Thule Neutron Monitor counts and sun spot numbers as a function of time.

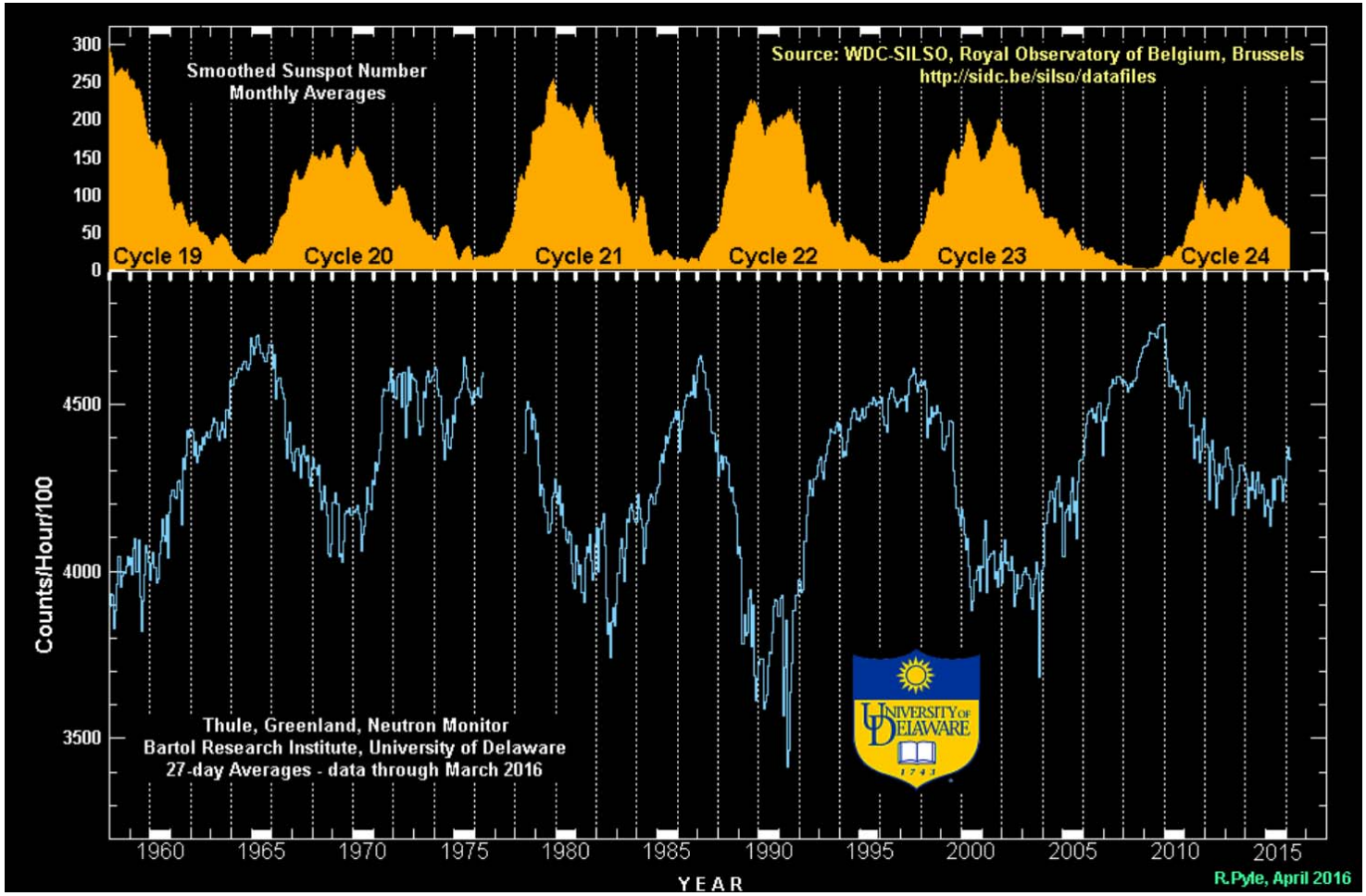

Sunspot number

Cosmic Rays as measured from the ground

A neutron monitor is a ground-based detector designed to continuously measure the number of cosmic rays striking the Earth's atmosphere.

As solar activity rises (top panel),
the count rate recorded by a neutron monitor decreases (bottom panel).

Balloon and space measurements of proton and He ion spectra

Curves are global fit - all experiments, times, p and He

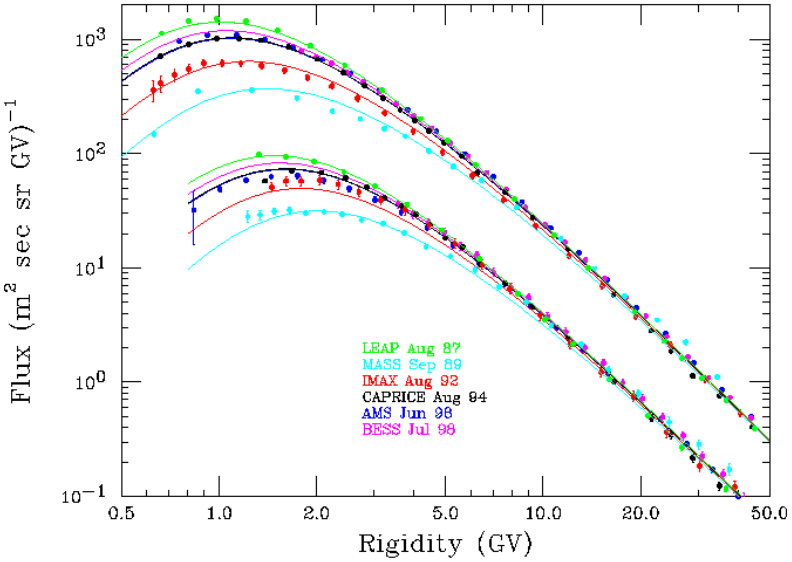

Fokker-Plank equation for the spherically symmetric model of the interplanetary medium, including only diffusion, convection and adiabatic acceleration

$$\frac{1}{r^2}\frac{\partial}{\partial r}\left(r^2\kappa\frac{\partial U}{\partial r}\right)-\frac{1}{r^2}\frac{\partial}{\partial r}(r^2VU)+\frac{1}{3}\left(\frac{1}{r^2}\frac{\partial}{\partial r}(r^2V)\right)\left(\frac{\partial}{\partial T}(\alpha TU)\right)=0$$

where $U(r,T,t)$ is the cosmic-ray number density per unit interval with kinetic energy T per nucleon, $\alpha=(T+2\cdot T_r)/(T+T_r)$, and T_r is proton's rest energy.

Diffusion Coefficient $\kappa \simeq \kappa_o(t)\kappa(r)(\beta R)$

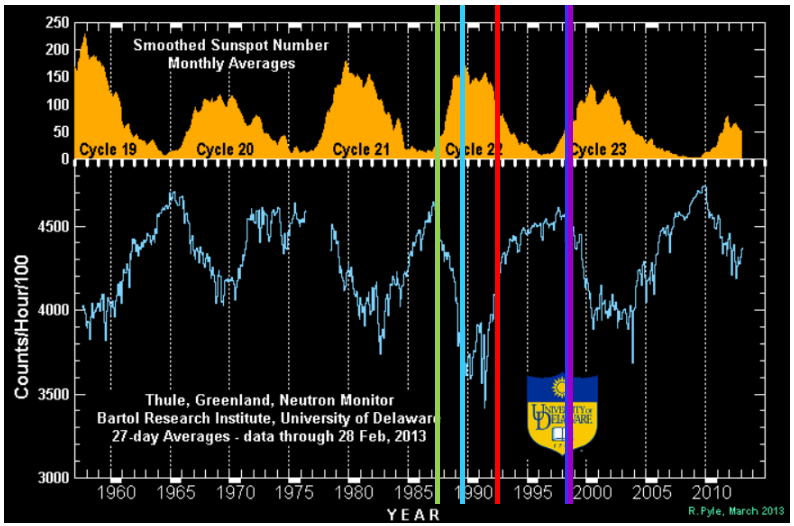

Thule Monitor count rates with times marked for above observations.
Same color code is used.

But there is a problem

Modulation theory can not predict the observed negative slope of low energy electron spectrum 20–200 MeV.

Based on solar electron observation it is expected the electron diffusion at low energies have much longer mean free paths than predicted. However incorporating this effect, the magnitude is still not enough to explain our observations

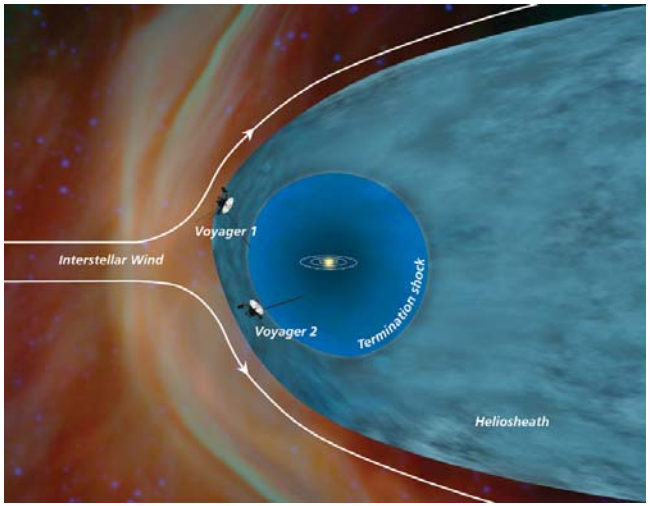

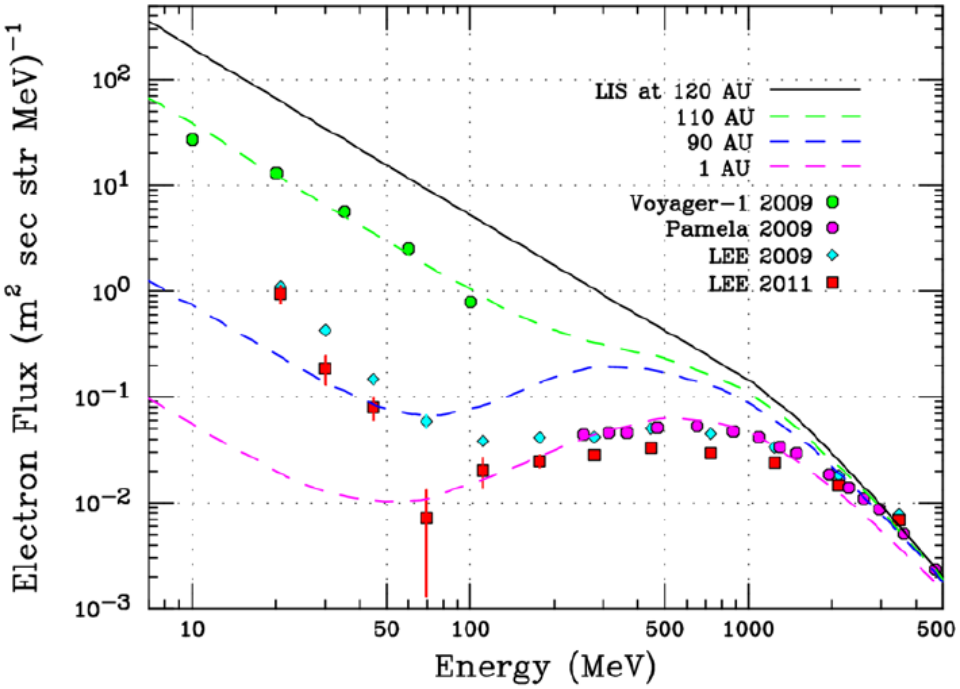

Estimate of the interstellar electron spectrum based on recent Voyager data (Potgeiter et al. 2013) compared with Pamela and LEE observations during 2009 (Evenson and Clem 2011) as well as 2011 LEE flight for comparison

Program Science Objectives

Past Observations of electrons in the energy range 10MeV to 5GeV.

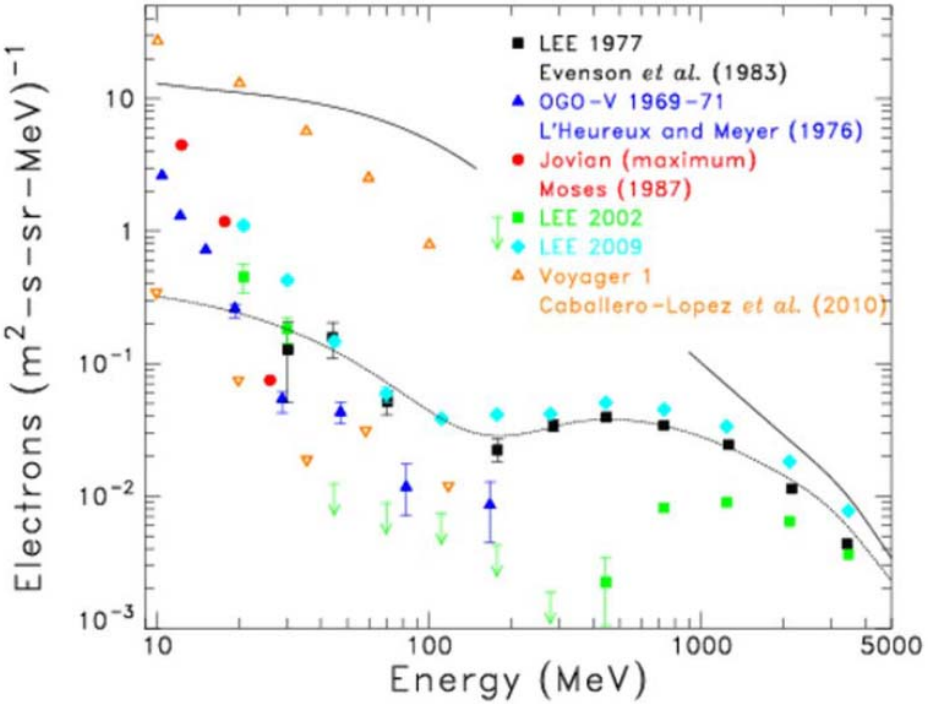

<u>Primary goal</u> of the AESOP-lite program is to measure primary electrons and positrons in the energy range of 20MeV to 300MeV

Observations of low energy electrons and positrons in the inner heliosphere simultaneously with Voyager will address three questions.

1. What causes the negative slope of the spectrum below 100MeV?
2. Why is the spectrum so variable within the outer heliosphere while it is apparently rather stable at 1 AU?
3. What is the source of these low energy electrons?

What is the origin of the low-energy turn-up in the cosmic-ray electron spectrum between ~10 and ~100 MeV, and what is the origin of these electrons?

Positrons typically constitute ~5% to ~30% of the total electron spectrum above 100 MeV and are generally believed to be of ‘‘ galactic secondary" origin due to decay chain pion --> muon --> positron.

1) A confirmed positron excess at low energy (above that expected from pion decay) would herald the discovery of primary positrons at low energies, presumably accelerated from ambient supernova material

2) If measurements indicate that the low-energy electron turn-up has a similar composition to that observed at several hundred MeV, the focus would be on models that explain why electron diffusion at low energies is inconsistent with standard modulation theory.

3) If the composition is below that expected from Galactic propagation, the source of the electron turn-up is likely local to the Heliosphere.

Payload Instrumentation

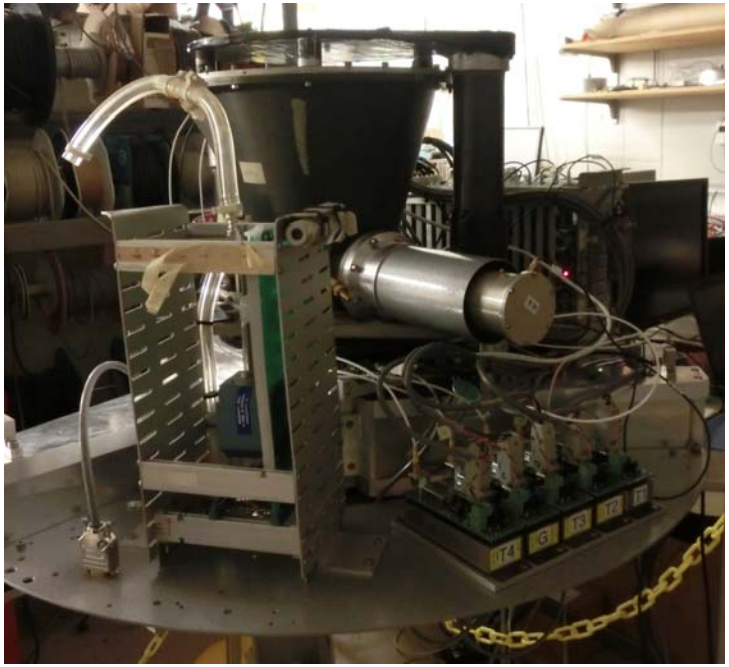

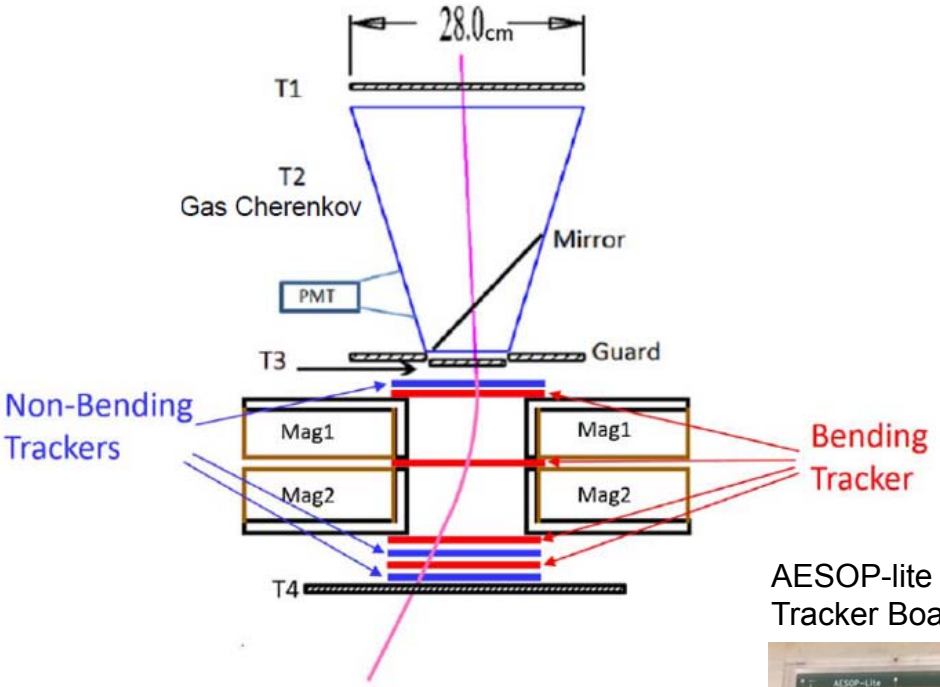

AESOP-lite SSD
Tracker Board

228 μm pitch

The instrument detects electrons and positrons with plastic scintillators **T1**, **T3** and **G** (anticoincidence) and the gas Cherenkov detector **T2**.

Seven planes of solid state strip detectors measure deflection in the field of dual permanent magnets.

AESOP-lite Summary

The origin of the turn-up in the cosmic ray electron spectrum below 100 MeV has been a mystery since cosmic-ray electrons were discovered in ~1960 and positron measurements can provide important information on its origin.

AESOP-Lite instrument is based on proven technology and it has the capability to make the best measurements to date to resolve this mystery by determining if there is evidence for primary positrons, or evidence that models for electron transport in the heliosphere are in need of revision.

On target to have a fully integrated instrument by late October this year and Palestine integration in February 2018 and flight from Sweden May 2018

Science Motivation for ANITA

Antarctic Impulsive Transient Antenna

Some background…..

ANtarctic Impulsive Transient Antenna

University of Hawaii at Manoa
Peter Gorham, PI
John Learned and Gary S. Varner

University of Delaware
John Clem , David Seckel
and Peng Cao

University College London
Ryan Nichol

Jet Propulsion Laboratory
Kurt Liewer, Charles Naudet
and Andres Romero-Wolf

University of Chicago
Abby Vieregg

University of California, Los Angeles
David Saltzburg and Stephanie Wissel

Ohio-State University
Jim Beatty and Amy Connelly

Washington University
Bob Binns and Marty Israel

University of Kansas
David Besson

National Taiwan University
Jiwoo Nam

A long time ago in a galaxy far, far away....

there was super-massive black hole at its center.

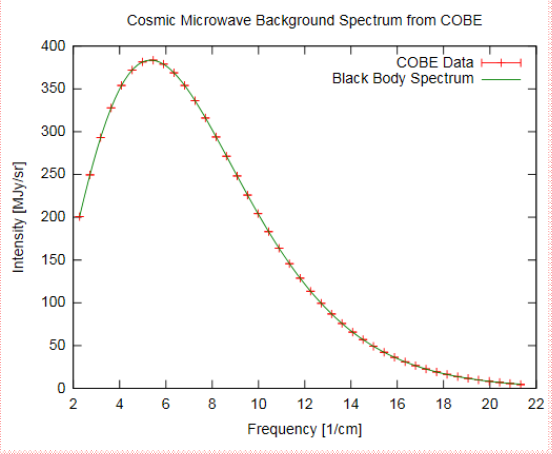

Microwave photons are Doppler shifted to ~GeV photons

Cosmic Microwave Background

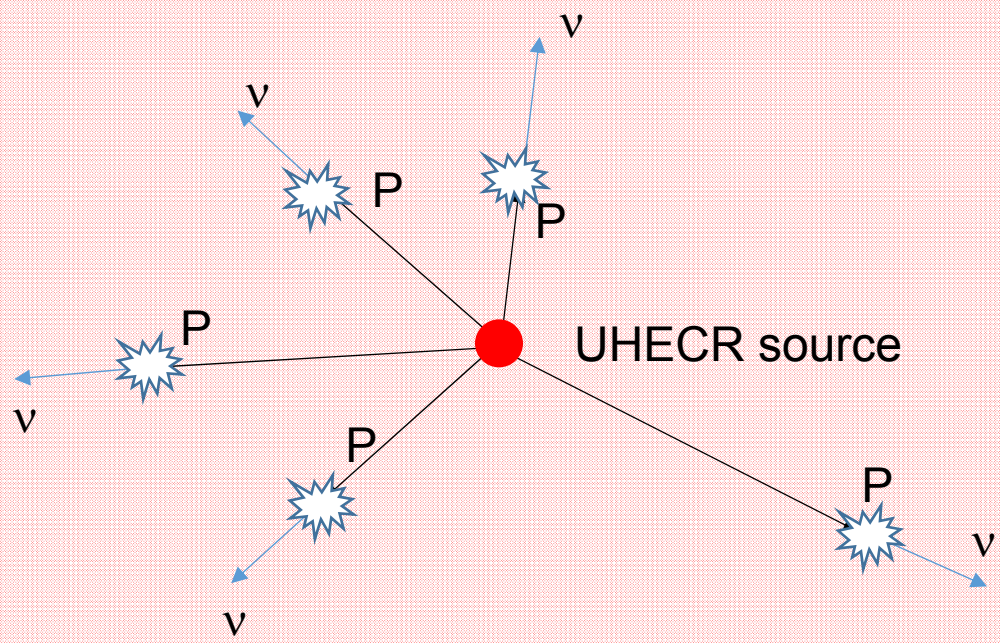

This process imposes a cutoff in the maximum energy of any hadronic UHECR particle as it propagates out from its source Greisen, Zatsepin and Kuzmin (GZK) cutoff.

What can we learn from studying EeV neutrinos?

If GZK (Greisen–Zatsepin–Kuzmin) process is the source of the UHE cutoff

$$\gamma_{\mathrm{CMB}} + p \rightarrow \Delta^{+} \rightarrow n + \pi^{+}$$

UHECR propagate through intergalactic space filled with the 3K cosmic microwave background radiation blue shifted to GeV gamma-ray energies in Rest frame

UHE neutrinos may be observed as byproducts of the GZK process, or they may be observed from the same astrophysical sources that produce UHECR.

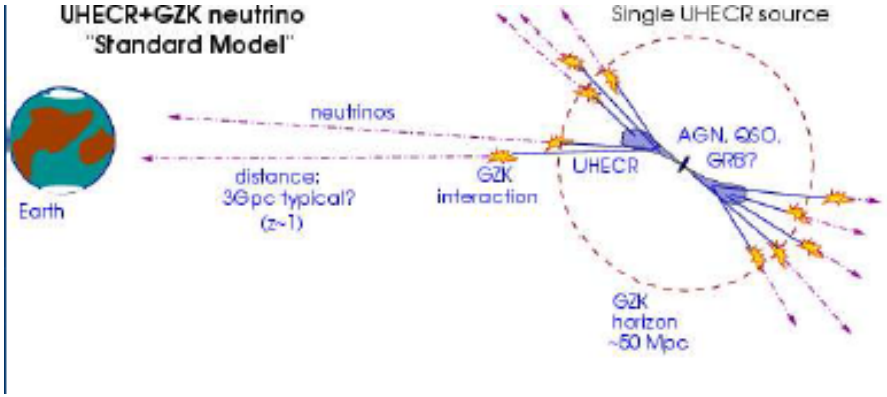

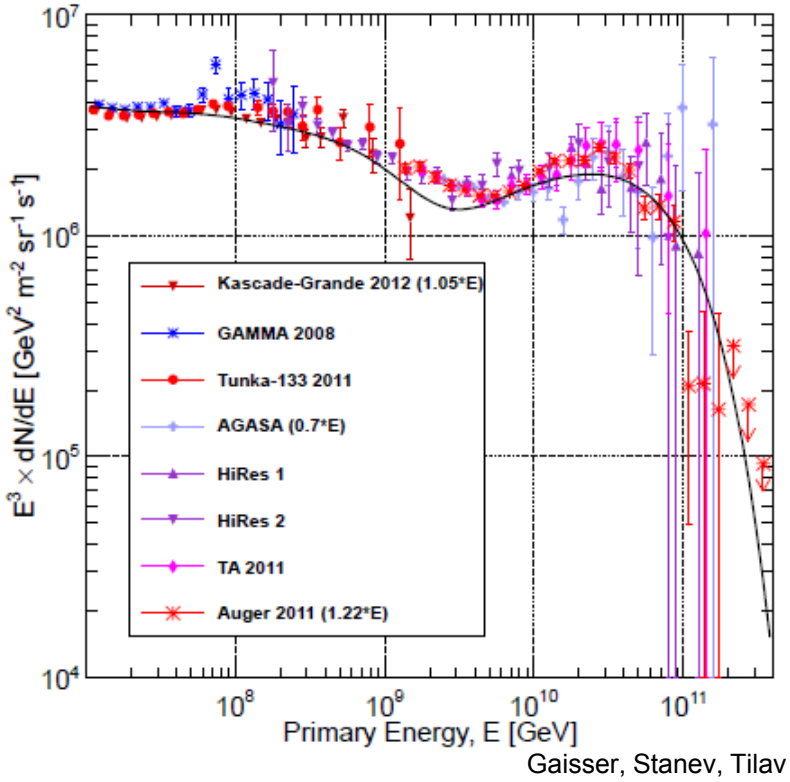

Gaisser, Stanev, Tilav

Cosmic ray data points to cutoff a GZK threshold

UHECR provide only **local** source information
Cosmic Accelerators likely to evolve in many ways: strength, composition, number density,
GZK neutrino spectra are direct from sources at all epochs

How can we measure EeV neutrinos?

Detection requires a target for conversion of the UHE neutrino to a high-energy particle cascade, followed by observation of electromagnetic radiation signatures from the the particle cascade.

Particle cascades result in an evolving population of electrons, positrons, and photons.
– Additional electrons are produced from knock-on collisions
– Positrons are depleted by in-flight annihilation.
– The net effect is a negative charge excess (~20%) in the shower moving relativistically.

Coherent Cherenkov Radiation at long wavelengths!

Particle cascade or "Shower" is actually a thin disk of HE particles
A few mm thick and few cm wide in solids

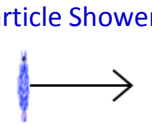

At wavelengths much greater than the shower radius, Cherenkov light adds coherently from all excess electrons.

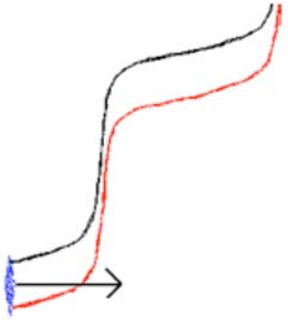

At smaller wavelengths Cherenkov light experiences destructive interference from electrons at different parts of the shower.

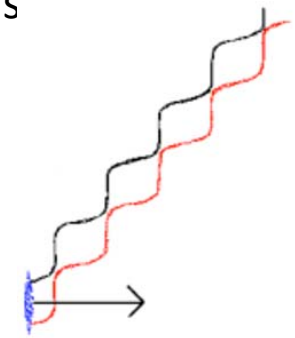

At radio wavelengths longer than ~10-20 cm:
appears as a single charge of $Z \sim 10^8$ → $Z^2 = 10^{16}$ x single e-

Askaryan effect: coherent Cherenkov EM wave

Select materials with long attenuation lengths in the RF have been tested at SLAC in a photon and electron beams.

silica

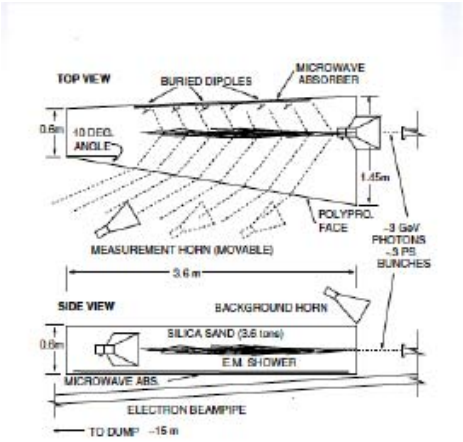

salt

ice

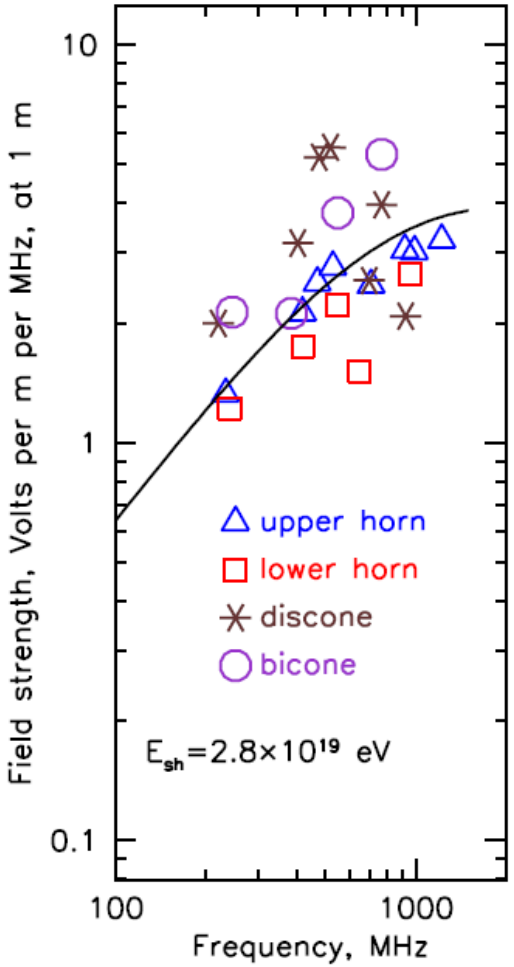

"Askaryan" effect has been confirm in these materials

For ANITA, the target is the Antarctic ice, which is observed from balloon altitudes.

The combination of the Antarctic polar vortex, providing excellent coverage of the large areas of very deep ice, and the remarkable radio-frequency clarity of ice leads to ANITA's essential methodology:

A radio-triggered waveform recorder using an antenna array to observe an effective target of order a million cubic km of ice in view at any time.

The radio emission from a neutrino-initiated cascade is beamed into a radio-Cherenkov ring, which must then point toward ANITA's direction for detection

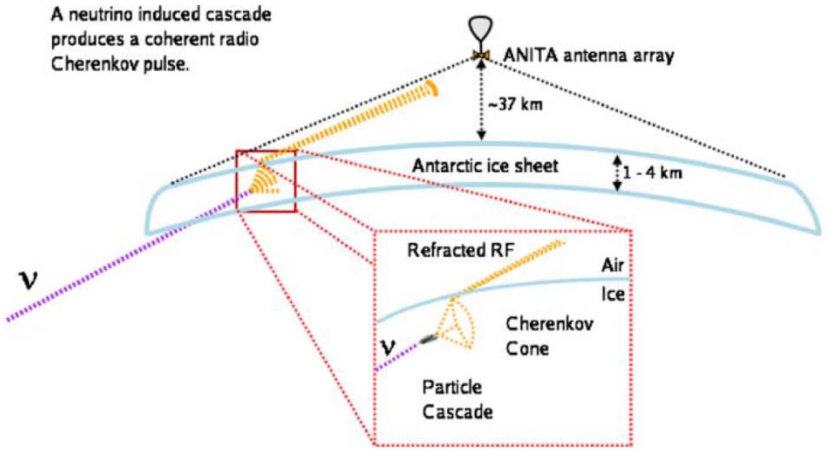

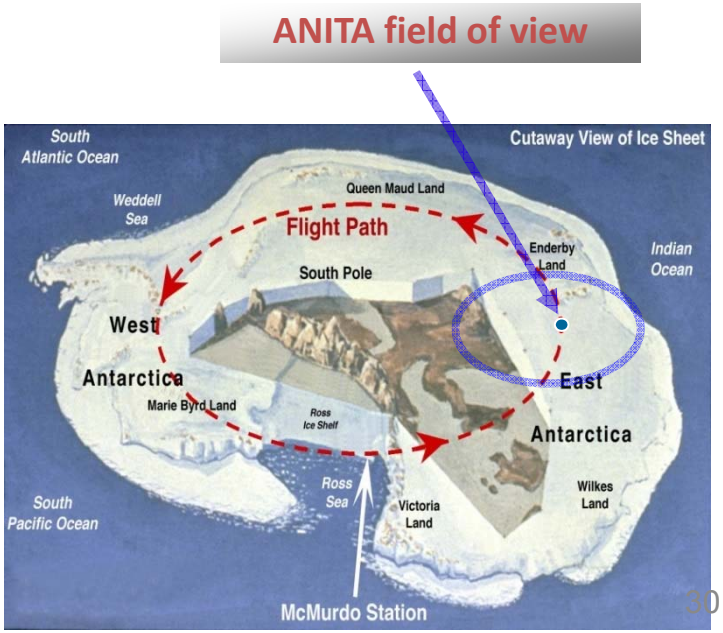

Polarization

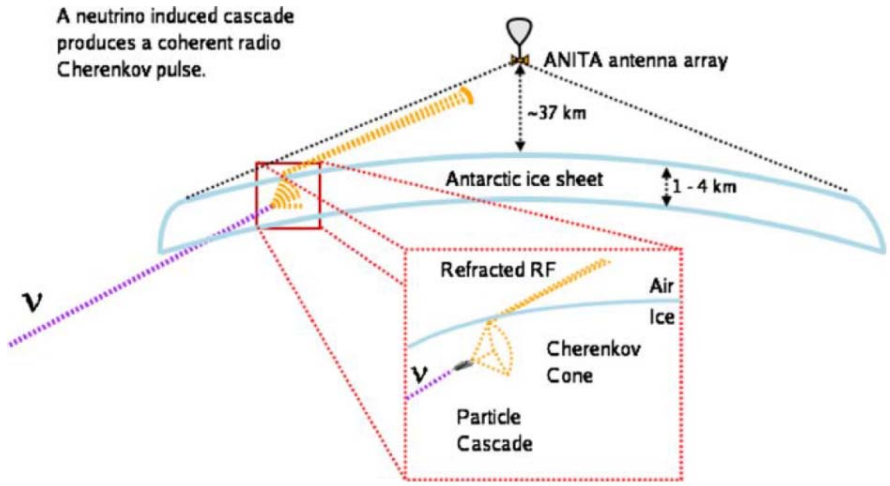

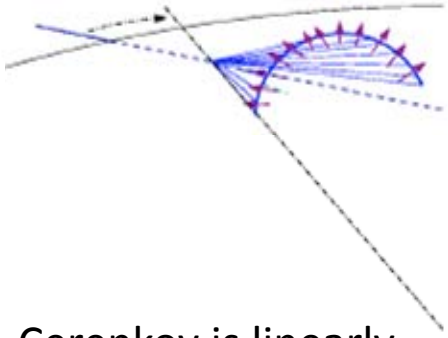

Cerenkov is linearly polarized perpendicular to cascade momentum and wave front

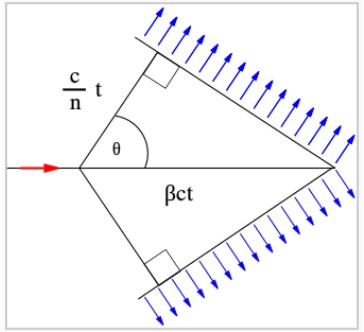

Only top portion of the cone escapes total internal reflection

Askaryan signals originating in the ice strongly favor vertical polarization

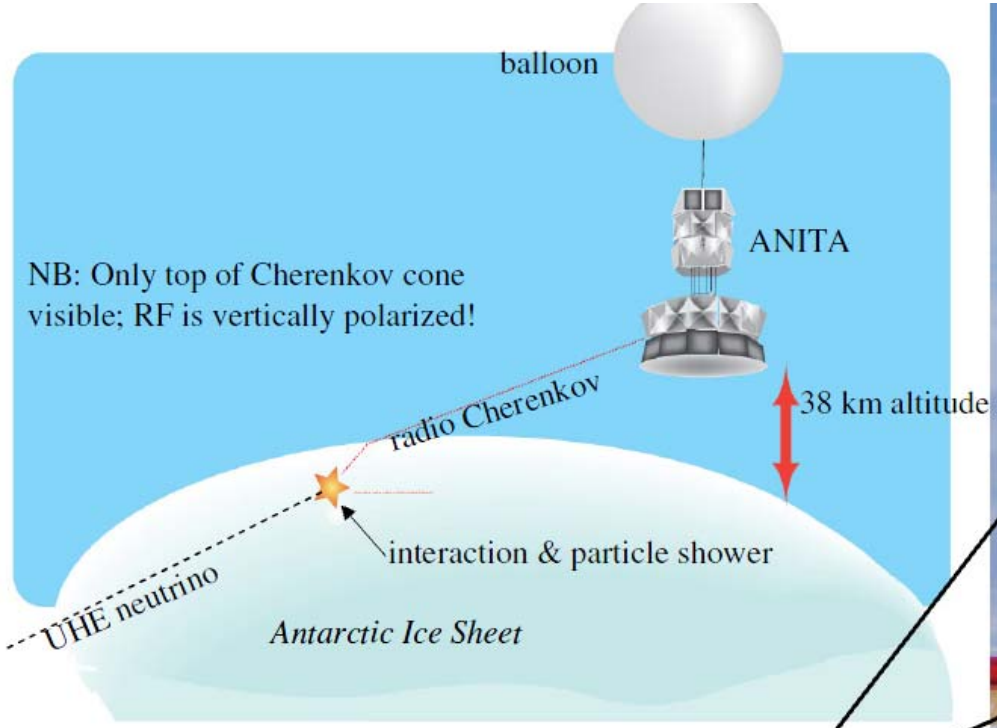

Stephen Hoover

A cartoon drawing of the ANITA concept: balloon with an array of radio antennas cylindrically arranged flies over the Antarctic continent, with the neutrino interaction and Cherenkov emission shown.

A photograph of the ANITA 1 balloon payload before launch in December 2006

ANITA is also sensitive to radio emission from ultrahigh energy cosmic ray extensive air showers

- EAS has e^- and e^+ moving through Earth's **B**-field
- Lorentz force → acceleration
  deflects the electrons and positrons in opposite directions.
- Acceleration → radio emission

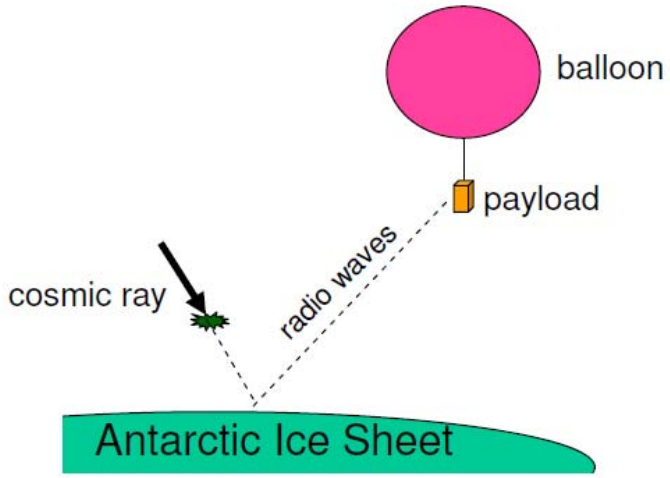

RF is polarized in the plane perpendicular to the Earth's B-field which is nearly vertical in Antarctica

Consequently Cosmic Ray signals strongly favor horizontal polarization

Example Events from ANITA4 flight Dec 2016

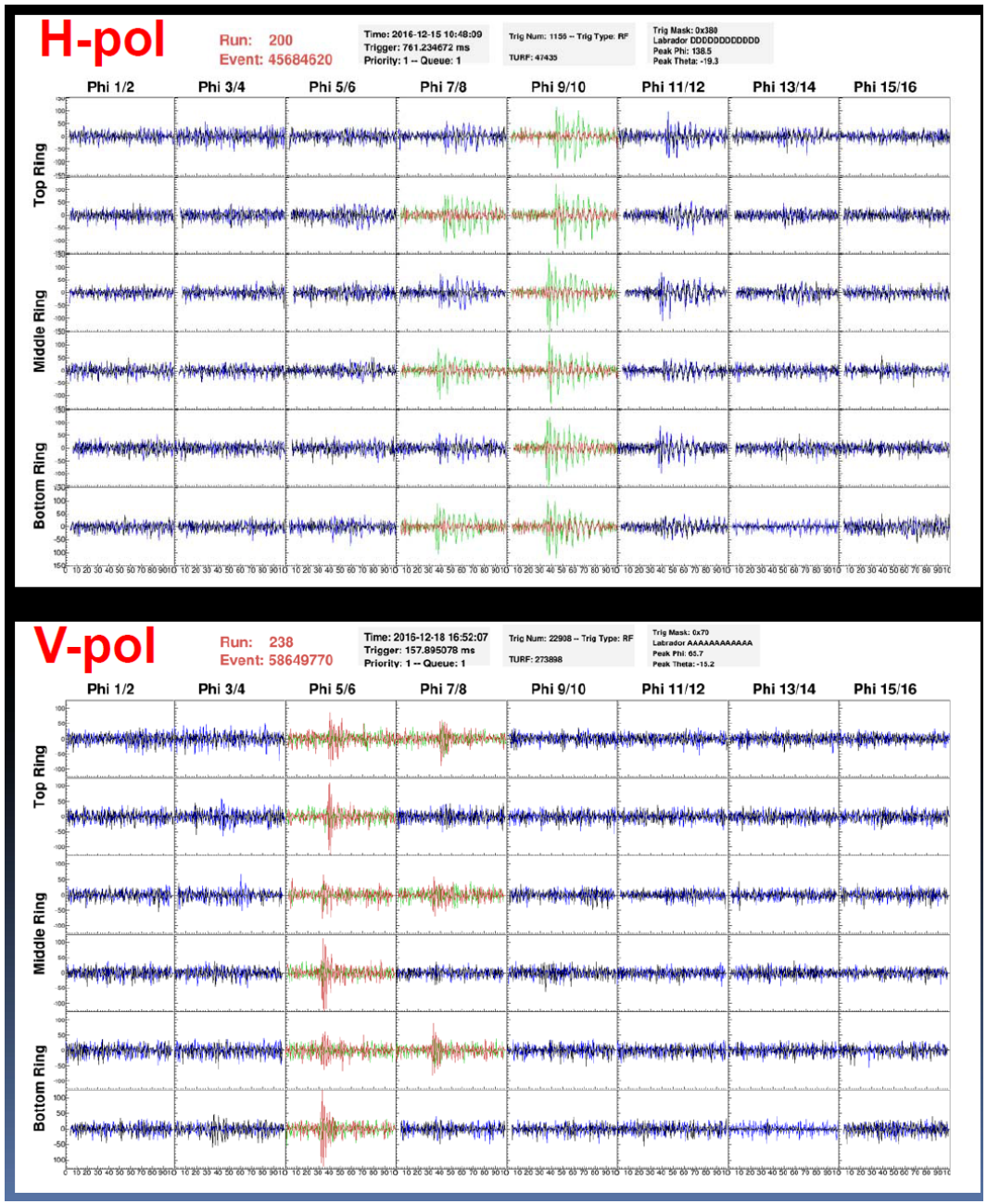

Single Phi Sector

Event Reconstruction

- **Angular reconstruction is a crucial part in the ANITA data analysis.**

Powerful background rejection

Incoherent thermal events (99% of data set)

Anthropogenic RF events from existing bases

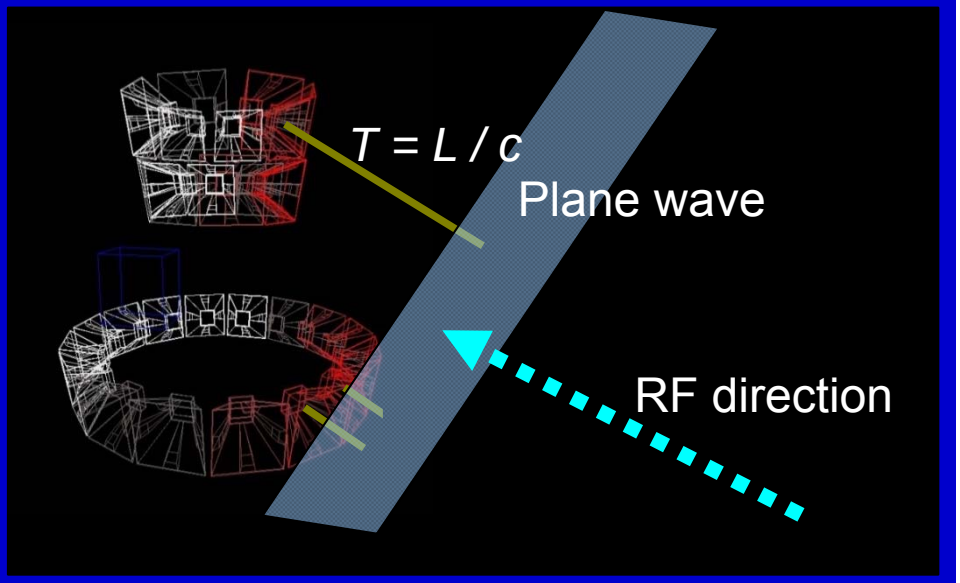

- **Angular reconstruction using Interferometry.**

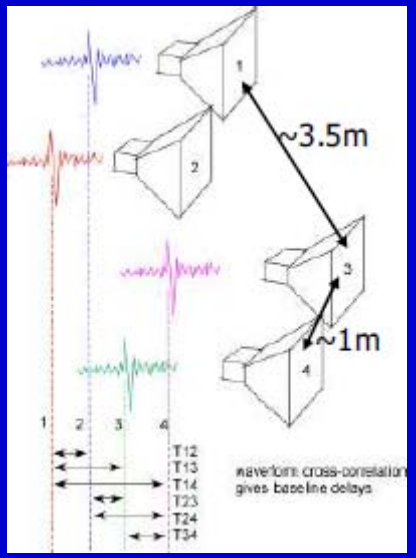

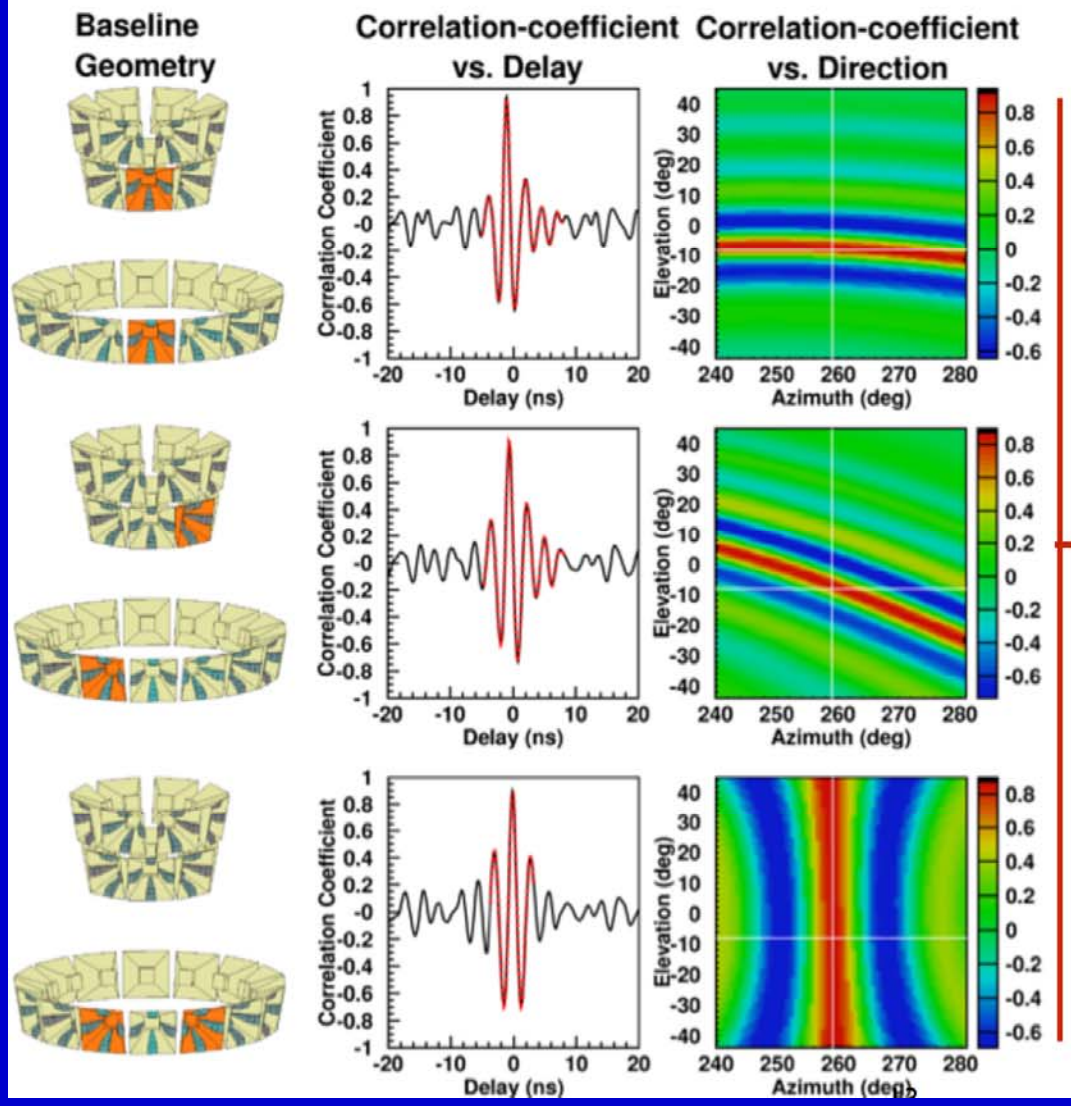

Correlate multiple antennas to "beat down" the noise

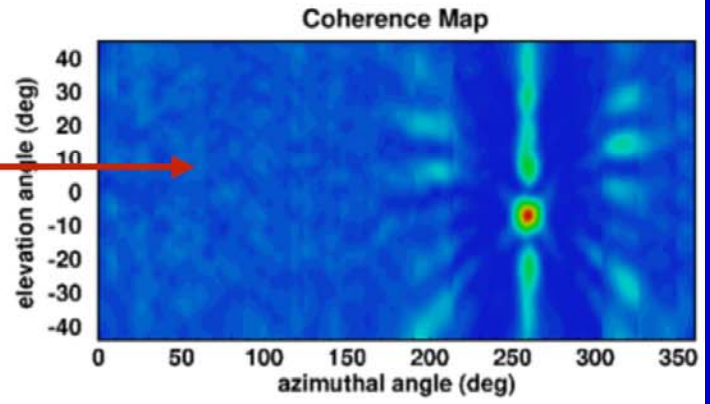

A. Romero-Wolf *et al (2013)*, arXiv: 1304.5663

Pointing Resolution

Signal comes from peak of interferometric image

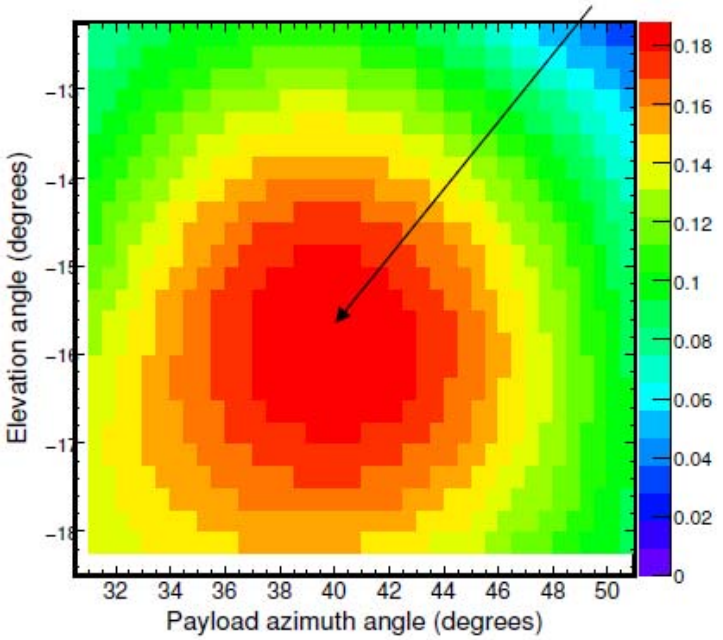

Pointing Error to Calibration Source

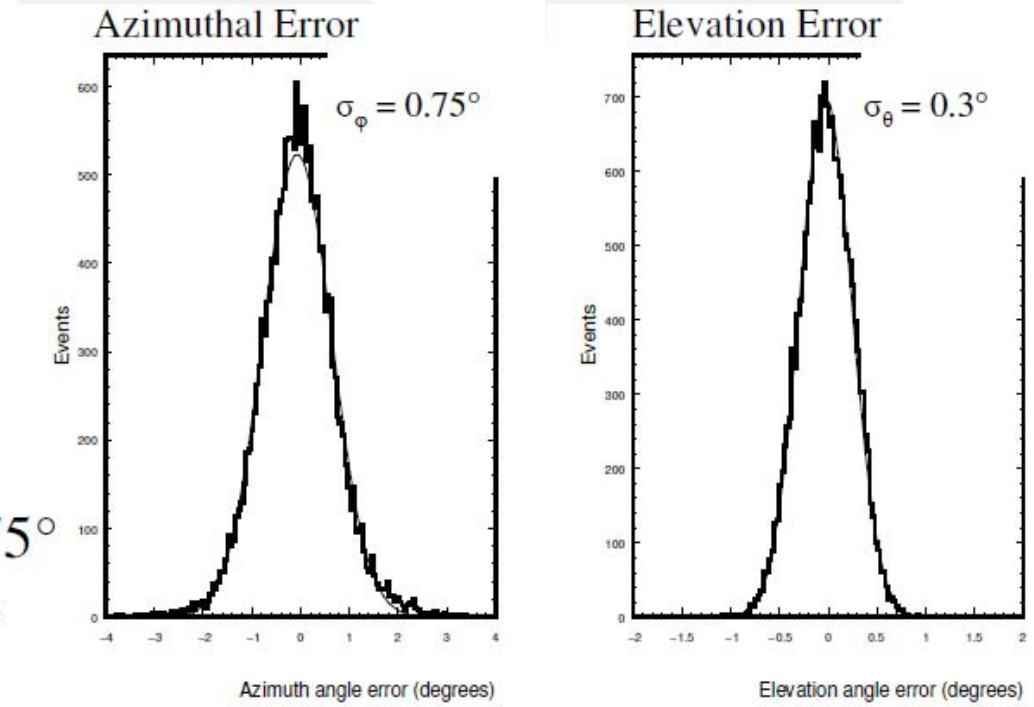

- Azimuthal resolution ~ 0.75°
- Elevation resolution ~ 0.3°

Prior ANITA Flights

ANITA-I (2006-2007) 35 days

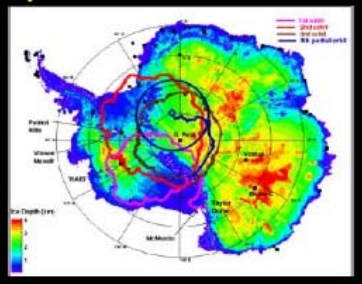

32 Antennas
Both H-pol/V-pol trigger
No neutrino candidate seen
Observation of 16 CR events
Observation of 1 up-coming event

ANITA-II (2008-2009) 30 days

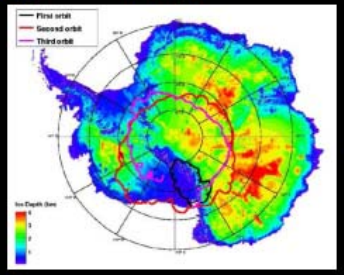

40 Antennas
V-pol trigger only
1 neutrino candidate observed
Additional 2 CR events

ANITA-III (2014-2015) 22 days

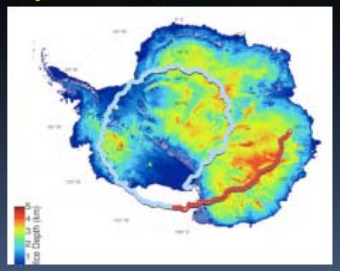

48 Antennas
H-pol/V-pol trigger

Data analysis in progress

Each flight increased the sensitivity with improved instruments

ANITA's signatures

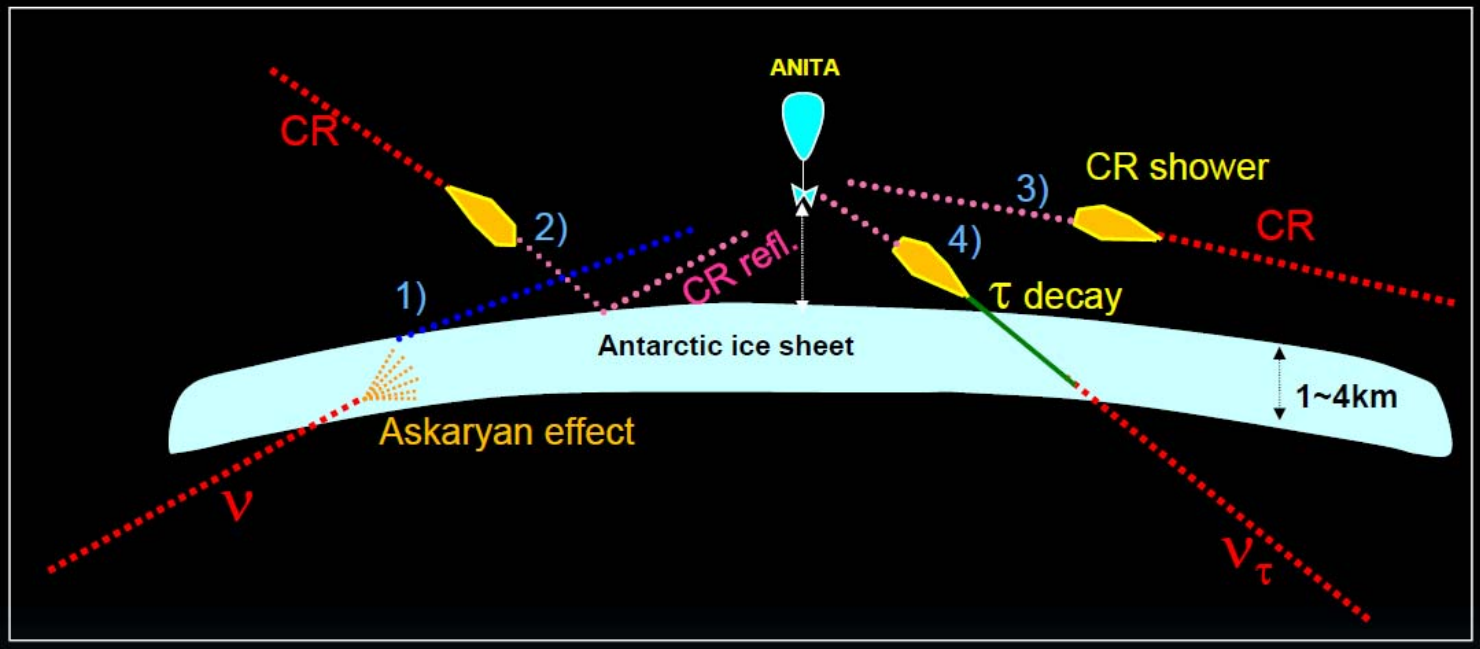

Origin	RF production	Polarization	RF Direction	Polarity
1) Neutrinos	Askaryan	V-pol	Below Horizon	Normal
2) CR-reflected	Geo-synchrotron	H-pol	Below Horizon	Inverted
3) CR-direct	Geo-synchrotron	H-pol	Above Horizon	Normal
4) Tau Neutrino?	Geo-synchrotron	H-pol	Below Horizon	Normal

ANITA-4 Instrument

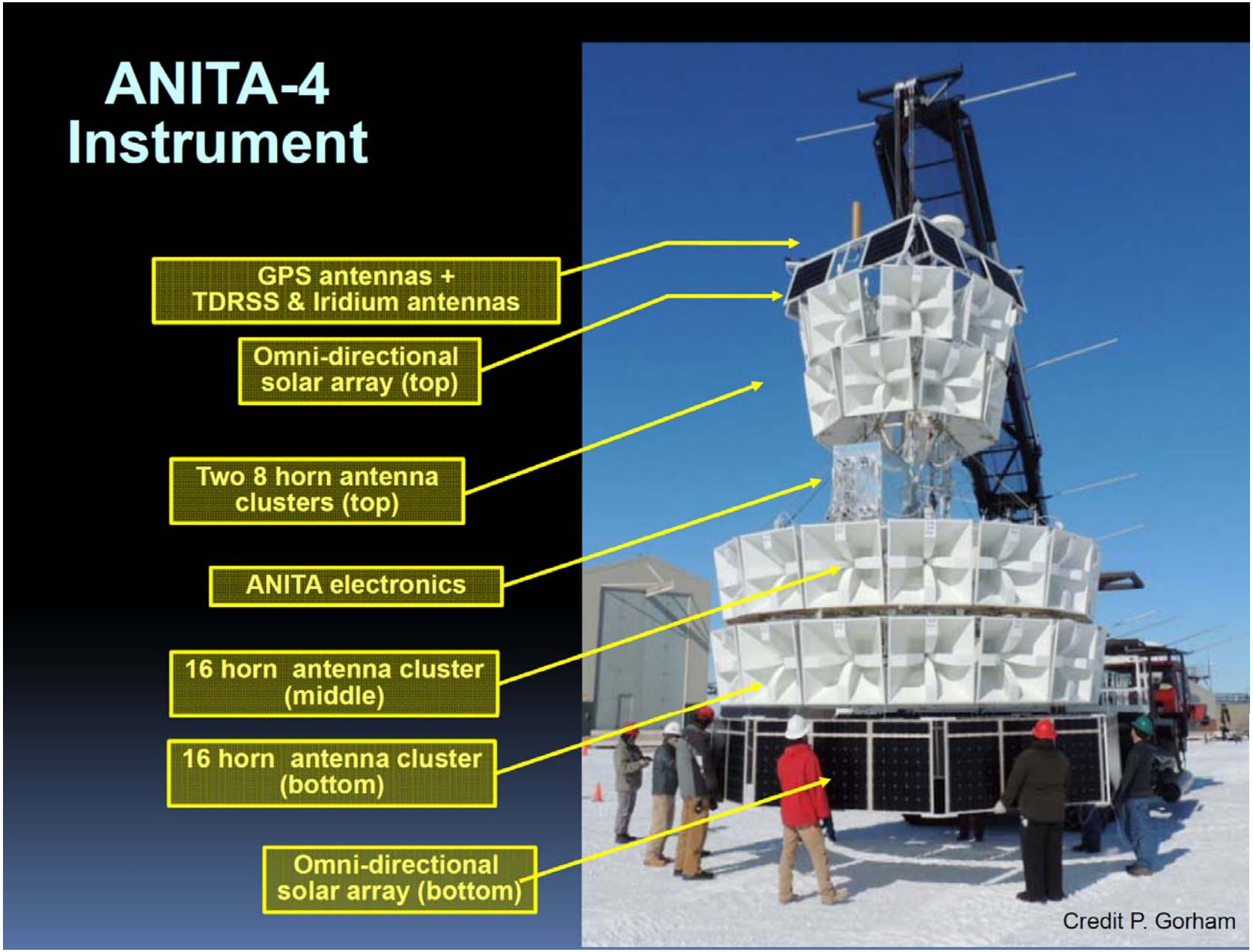

ANITA-4 Flight

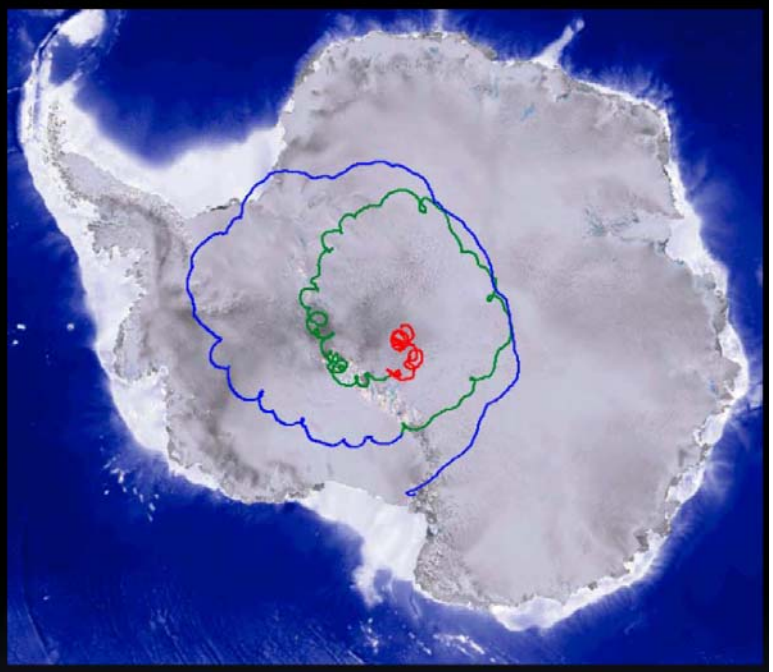

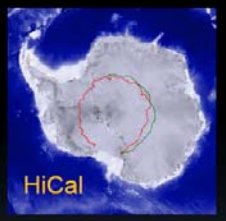

Launched on December 2nd 2016 at Williams Field, Antarctica
Landed on December 30 2016 near South Pole (232 km away)
→ **28 days at float**
A spiral pattern of trajectory: keep away from McMurdo Station (highest noise source)
Two follow-up payloads (HiCal) were also launched

ANITA UHECR Events

PRL 105, 151101 (2010)

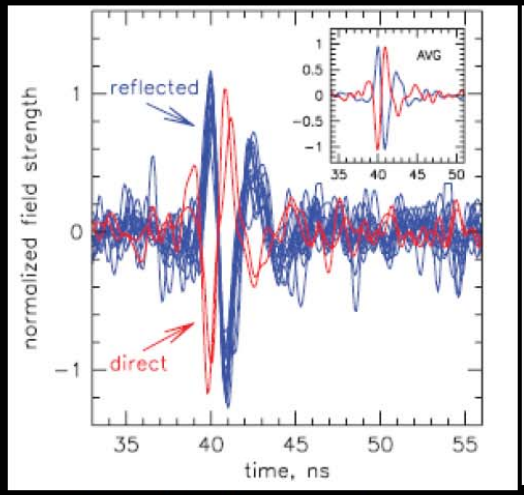

Unfolded waveforms

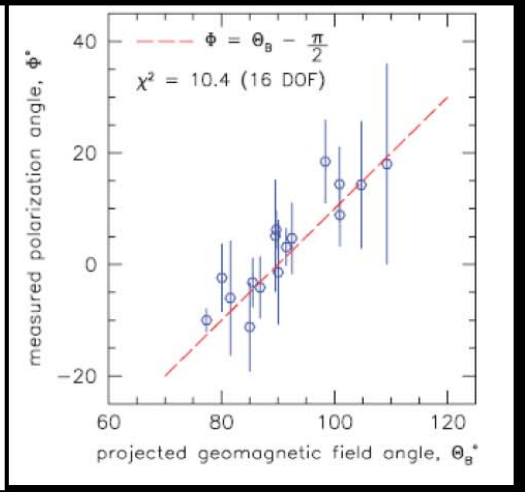

Geomagnetic field correlation

16 UHECR Events :
14 reflected + 2 direct from ANITA-I
2 events from ANITA-II
→ H-pol trigger was off (optimized for neutrino)

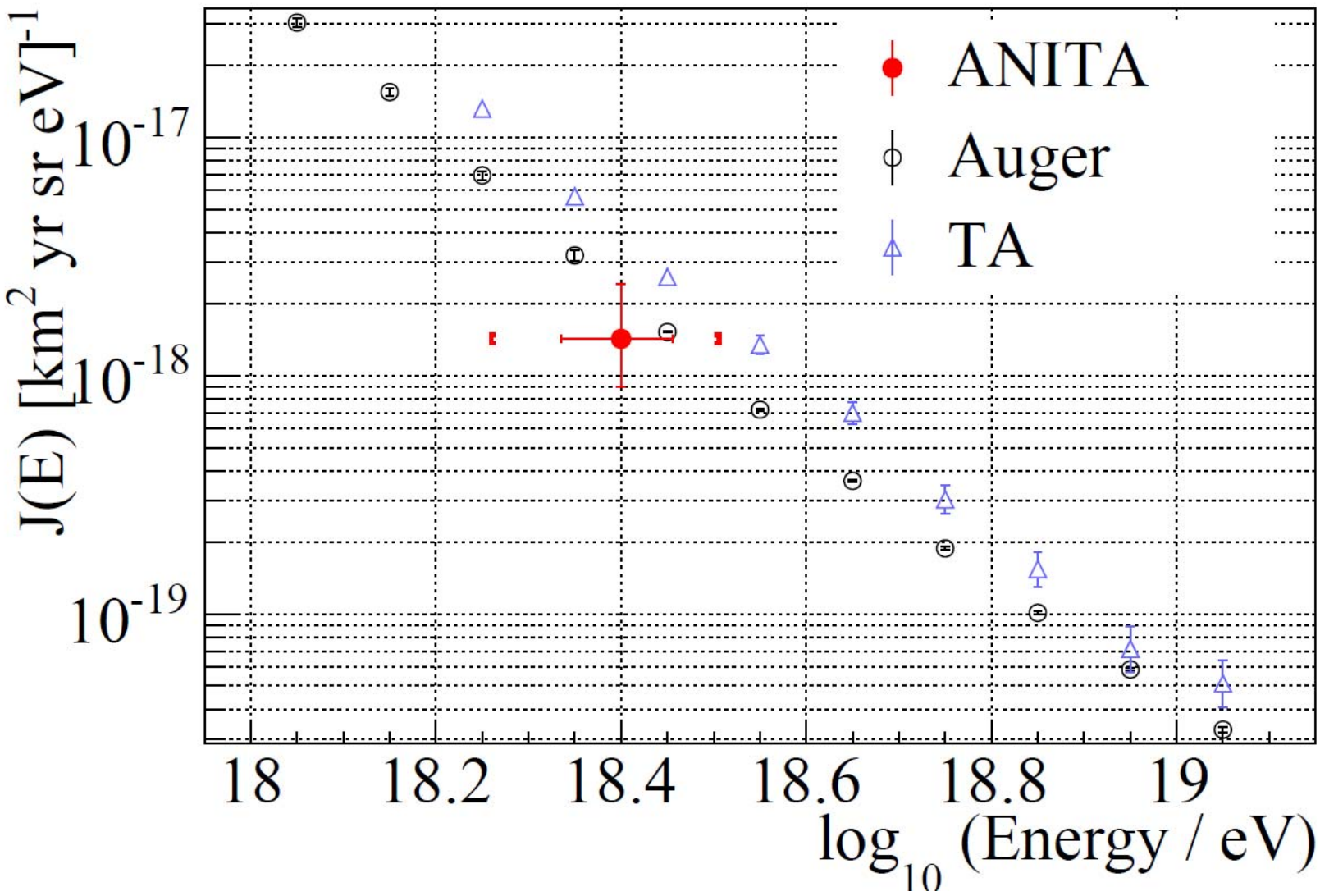
ANITA
Auger
TA
J(E) [km^2 yr sr eV]$^{-1}$
10^{-17}
10^{-18}
10^{-19}
18
18.2
18.4
18.6
18.8
19
$\log_{10}$ (Energy / eV)

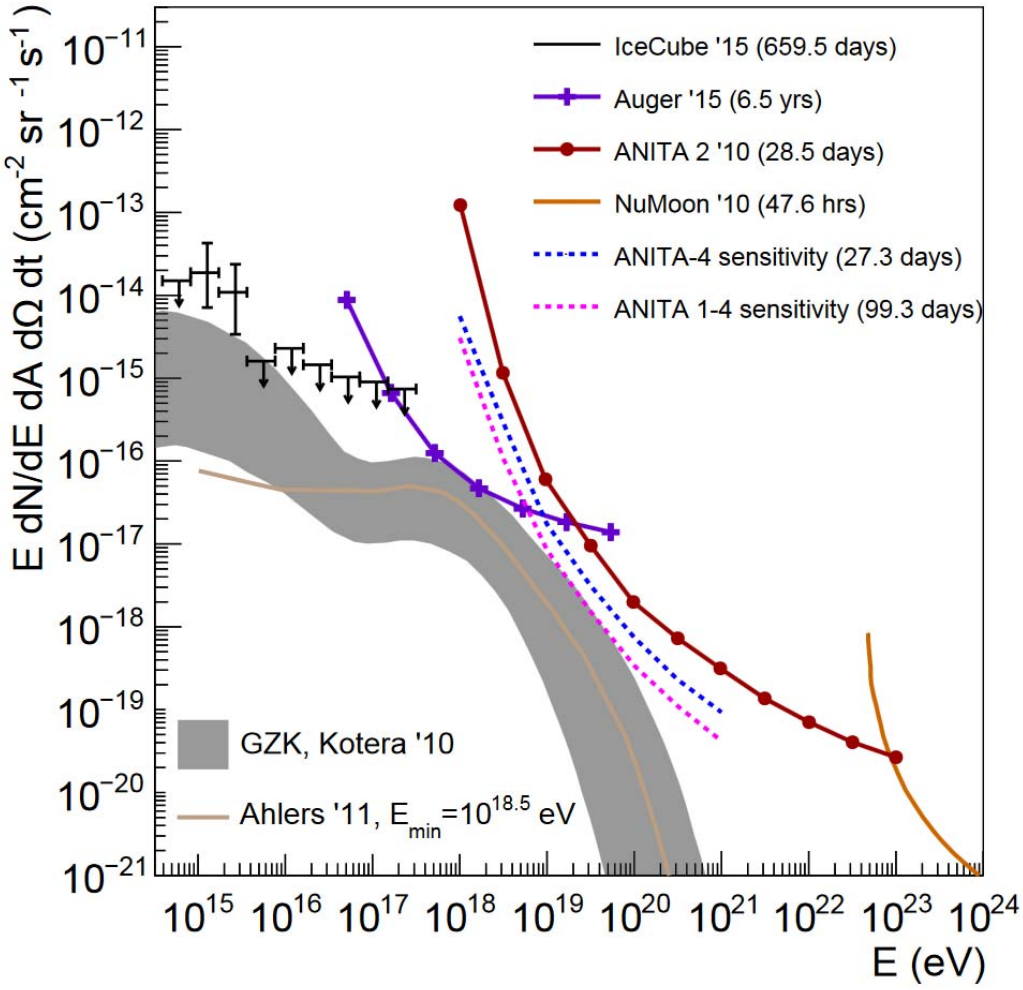

ANITA: Best constraints for $E_\nu \gtrsim 10_{19}$ eV

Differential limits on the flux of cosmogenic neutrinos set by IceCube, Auger, ANITA 2, NuMoon, ANITA 4 and ANITA1-4 Flux model predictions for GZK cosmogenic neutrinos.

Summary & Plan

ANITA successfully completed the fourth flight with improved performance;

- 20% lower energy threshold
- Factor 3.6 increased exposure

Data analysis of ANITA-3 and ANITA-4 in progress
- well positioned for neutrino discovery!
- hundreds of CR events expected!